Lithuanian Journal of Physics, Vol. **58**, No. 3, pp. 254–260 (2018)

THE GROWTH, STRUCTURE AND LUMINESCENCE PROPERTIES OF $ZnSe_{1-x}S_x$ MATERIALS

O.G. Trubaieva [a], M.A. Chaika [b], and A.I. Lalayants [a]

[a] *Institute for Scintillation Materials NASU, Nauki Ave. 60, 61072 Kharkov, Ukraine*

[b] *Institute of Physics PAS, al. Lotników 32/46, PL-02-668 Warsaw, Poland*

Email: trubaeva.olya@gmail.com

Received 2 December 2017; revised 19 February 2018; accepted 21 June 2018

$ZnSe_{1-x}S_x$ crystals with a higher content of selenium or sulfur ions adopt, respectively, a wurtzite or sphalerite structure. Luminescent properties of $ZnSe_{1-x}S_x$ crystals are determined by ternary $V_{Zn}Zn_iO_{Se}$ complexes for crystals with a cubic (sphalerite) lattice, and by sulfur vacancies V_S for crystals with a hexagonal (wurtzite) lattice. Light output of $ZnSe_{1-x}S_x$ crystals increases with increasing the sulfur content up to $x = 0.3$ and reaches the value of light output observed for 'classic scintillator' ZnSe(Te). At the same time, the $ZnSe_{1-x}S_x$ bulk crystals possess better thermal stability at the same energy of emitted photons ($h\nu \sim 2$ eV) as compared to that of the ZnSe(Te) crystals.

Keywords: mixed crystals, $ZnSe_{1-x}S_x$, radiation detector, scintillator, X-ray induced luminescence

PACS: 78.20.-e

1. Introduction

Up to now, the possibility of obtaining scintillation materials based on A^2B^6 mixed crystals (ZnS-ZnTe) has been shown [1–6]. A^2B^6 mixed crystals have found many applications, first of all, in development of detecting devices for introscopic systems and in multi-energy X-ray radiography [4, 7]. A low value of the effective atomic number for ZnS crystals sufficiently limits their use as scintillating materials [8]. On the other hand, the variation of the band gap width opens possibilities for obtaining ZnS-based materials with pre-determined scintillation properties [9, 10].

Obtaining of ZnS_xTe_{1-x} mixed crystals is difficult due to the limited solubility of their components and is possible only at 8–10% concentrations in accordance with the ZnS_xTe_{1-x} state diagram [11, 12]. Among various A^2B^6 solid solutions, $ZnSe_{1-x}S_x$ crystals are of especial interest. Unlimited ZnS-ZnSe mutual solubility makes possible obtaining of a $ZnSe_{1-x}S_x$ crystal with any x value [13, 14]. The change of the ZnS/ZnSe ratio for $ZnSe_{1-x}S_x$ single crystals opens a wide range of possibilities for tuning their properties, including scintillation ones [14–17]. Moreover, $ZnSe_{1-x}S_x$ crystals have better transparency to their own radiation. The position of the energy levels of radiative recombination centres in the band gap of $ZnSe_{1-x}S_x$ crystals can be easily changed [18, 19]. There are different methods to obtain $ZnSe_{1-x}S_x$ mixed crystals, most of them using vapour phase growth methods [20] and only a few concern the directional solidification techniques which allow obtaining large $ZnSe_{1-x}S_x$ mixed crystals [21–23].

In this work the growth, structure and luminescence properties of $ZnSe_{1-x}S_x$ crystals depending on the concentration x are discussed. The properties of mixed $ZnSe_{1-x}S_x$ crystals were compared with those of the classical ZnSe(Te) scintillators widely used as X-ray and gamma detectors.

2. Experiment

Solid-state reaction (SSR) and directional solidification (DS) methods were used for obtaining $ZnSe_{1-x}S_x$ mixed crystals. $ZnSe_{1-x}S_x$ samples with five different initial compositions were obtained by the solid-state reaction method. Samples with 5, 25, 50, 75 and 95 wt.% of ZnSe are denoted as SSR-$ZnSe_{0.03}S_{0.97}$, SSR-$ZnSe_{0.18}S_{0.82}$, SSR-$ZnSe_{0.4}S_{0.6}$, SSR-$ZnSe_{0.67}S_{0.33}$, and SSR-$ZnSe_{0.93}S_{0.07}$, respectively. The solid-state reaction took place in the gradient zone of a muffle furnace with the following sintering conditions: T = 1273 K, t = 7 h, hydrogen atmosphere.

$ZnSe_{1-x}S_x$ bulk crystals were grown by the Bridgman–Stockbarger (directional solidification) method in graphite crucibles under inert conditions. The growth temperatures (T_{growth}) were in the range from 1853 to 1903 K depending on the melt composition. The corresponding samples are denoted as DS-ZnSe, DS-$ZnSe_{0.95}S_{0.05}$, DS-$ZnSe_{0.75}S_{0.25}$, DS-$ZnSe_{0.7}S_{0.3}$, DS-$ZnSe_{0.6}S_{0.4}$ and DS-ZnS. Annealing in zinc vapour (T = 1224 K, R = (3–5)·10^4 Pa, t = 48 h) was used in order to form luminescent centres and to inhibit nonradiative relaxation channels by excited charge carriers.

The chemical analysis of $ZnSe_{1-x}S_x$ powders was carried out in order to determine their chemical composition. The selenium content was controlled by means of an atomic emission spectroscopy (AES) spectrometer Trace Scan Advantage *Thermo Jarrell Ash*. The afterglow level η(%) was measured by means of a measuring-computing system for the determination of kinetic characteristics. The system consisted of a RAPAN-200 (E_{ex} = 100–160 keV) pulsed X-ray emitter, S8594 photodiode, current–voltage converter (IUC), multiplexer (MUX), controller, analog-to-digital converter (ADC), personal computer, oscilloscope (C1-102) and an X-ray emitter control unit (BCX).

Scintillation emission spectra were measured under X-ray excitation using a REIS-I (Cu, U = 10–45 kV) X-ray source. Luminescence spectra were measured by a KSVU-23 spectrophotometer. Measurements of relative light output were performed using an X-ray tube with a tungsten anode and a PD-24 *Smiths Heimann* AMS-1 silicon photodiode. Transmittance spectra were measured using a single-beam *Shimadzu* UVmini-1240 spectrophotometer.

3. Results and discussion

The directional solidification method is rather expensive, so before crystal growth the optimal range of x for $ZnSe_{1-x}S_x$ should be chosen. Therefore, the SSR method was used to study the effect of the sulfur content on the properties of $ZnSe_{1-x}S_x$ crystals in the entire range of x.

3.1. Powders

Even a small concentration of uncontrollable impurities can change significantly the properties of sintering samples. Therefore, the chemical analysis of the initial powders and the SSR-$ZnSe_{0.4}S_{0.6}$ sample was provided (Table 1). The concentration of uncontrollable impurities was practically the same for the initial powders and SSR-$ZnSe_{0.4}S_{0.6}$ sample except for the Si concentration. The solid-state reaction took place in a quartz boat leading to unavoidable Si inclusions in our sample. However, the Si content in our samples was less than 0.01 wt.%.

The normalized X-ray luminescence spectra of the $ZnSe_{1-x}S_x$ powders with a different ratio of components are shown in Fig. 1. All luminescence spectra of the SSR-$ZnSe_{1-x}S_x$ samples with a wurtzite crystallographic structure consist of a single luminescence band with a maximum in the range from 500 to 530 nm (Fig. 1). The decrease of the sulfur content leads to the shift of the luminescence band maximum to the long-wavelength region. These luminescence bands can

Table 1. Data of chemical analysis.

Sample	Content of element, weight %							
	Fe	Si	Mg	Ni, Bi	Al	Cu	Mn	Cr
ZnS	0.0005	<0.001	0.0005	<0.0001	0.001	0.00005	<0.00005	<0.0001
ZnSe	0.0001	<0.001	0.0001	0.0001	0.0005	0.00005	0.00005	<0.0001
SSR-$ZnSe_{0.4}S_{0.6}$	0.0008	0.01	0.0005	<0.0001	0.0015	0.00025	0.00015	0.0001

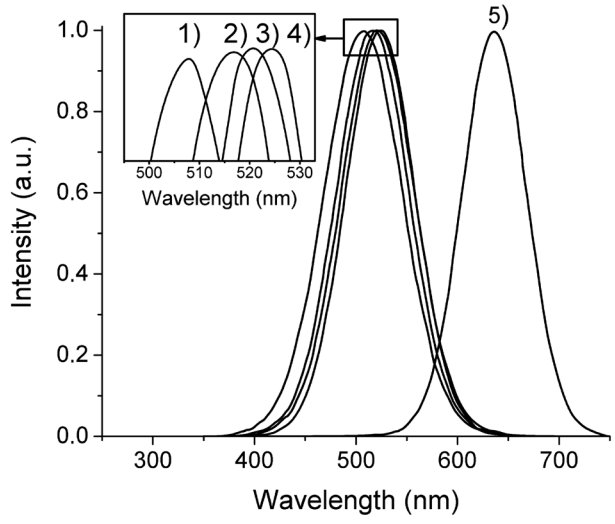

Fig. 1. X-ray luminescence spectra for the $ZnSe_{1-x}S_x$ powders obtained by the SSR method: SSR-$ZnSe_{0.03}S_{0.97}$(1), SSR-$ZnSe_{0.18}S_{0.82}$(2), SSR-$ZnSe_{0.4}S_{0.6}$(3), SSR-$ZnSe_{0.67}S_{0.33}$(4), SSR-$ZnSe_{0.93}S_{0.07}$(5).

be related to the recombination of electrons from the conduction band to V_S acceptor levels [24–26]. The change of the luminescence band maximum position is related to the shift of the fundamental absorption edge to longer wavelengths with the increase of the Se content [14, 27]. Further decrease of the sulfur concentrations leads to the wurtzite–sphalerite transition for SSR-$ZnSe_{1-x}S_x$ samples and a significant shift of the luminescence band maximum to the long-wavelength region (λ_{max} = 635 nm, Fig. 1, Curve 5). These luminescence bands can be associated with the ternary $O_{Se}V_{Zn}Zn_i$ complexes, which act as centres of radiation [18].

The afterglow determines the energy resolution and the speed of the detector. The largest afterglow level was observed for the SSR-$ZnSe_{0.03}S_{0.97}$ sample reaching 11.18% after 3 ms (Table 2). We suppose that the largest afterglow of SSR-$ZnSe_{0.03}S_{0.97}$ is related to a larger concentration of free electrons that do not participate in recombination [28]. A further increase of the selenium content leads to the decrease of the afterglow, due to the formation of acceptor centres, which act as the capture centres of free electrons [24, 25]. The lowest value of the afterglow was detected for the SSR-$ZnSe_{0.93}S_{0.07}$ samples (about 0.2%).

3.2. Bulk crystal

Data processing was carried out using the FullProf 3.0 program. The Rietveld analysis was applied to the 2θ XRD pattern of the $ZnSe_{1-x}S_x$ powdered crystals (Fig. 2). According to the X-ray diffraction (XRD) results, all $ZnSe_{1-x}S_x$ crystals possess sphalerite-type cubic lattices without any additional peaks.

Luminescence spectra of the $ZnSe_{1-x}S_x$ bulk crystals (x = 0.05–0.4) were investigated (Fig. 3).

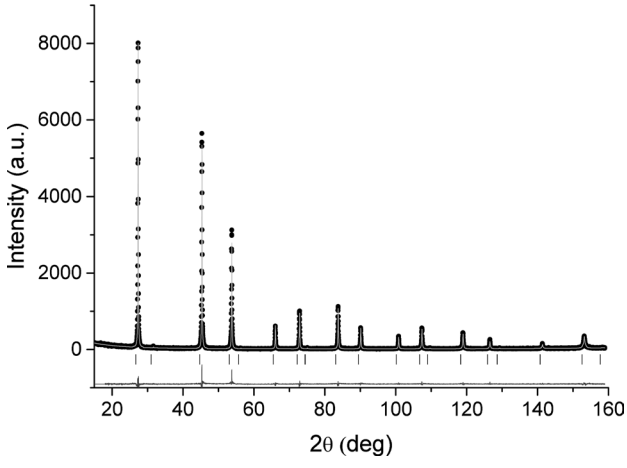

Fig. 2. Results of the Rietveld refinement for the powder diffraction pattern of the DS-$ZnSe_{0.95}S_{0.05}$ crystal. The upper points indicate the experimental and the solid line is the calculated pattern. The difference pattern is shown in the lower part of the figure.

Table 2. Data for the afterglow of the $ZnSe_{1-x}S_x$ samples obtained by SSR.

Composition	Phase composition	Afterglow %			
		3 ms	5 ms	10 ms	20 ms
SSR-$ZnSe_{0.03}S_{0.97}$	wurtzite	11.18	9.83	8.26	6.97
SSR-$ZnSe_{0.18}S_{0.82}$	wurtzite	2.97	2.64	2.25	1.92
SSR-$ZnSe_{0.4}S_{0.6}$	wurtzite	2.97	2.64	2.25	1.92
SSR-$ZnSe_{0.67}S_{0.33}$	wurtzite	0.26	0.24	0.23	0.21
SSR-$ZnSe_{0.93}S_{0.07}$	sphalerite	0.37	0.29	0.2	0.14

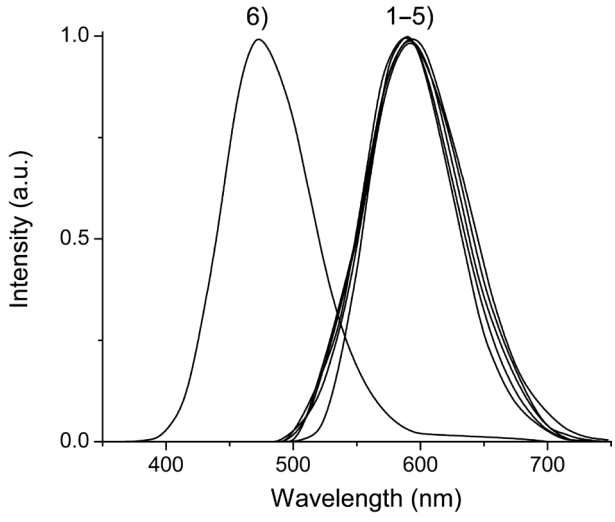

Fig. 3. X-ray luminescence spectra for the $ZnSe_{1-x}S_x$ crystals obtained by the DS method: DS-$ZnSe_{0.6}S_{0.4}$ (1), DS-$ZnSe_{0.7}S_{0.3}$ (2), DS-$ZnSe_{0.75}S_{0.25}$ (3), DS-$ZnSe_{0.95}S_{0.05}$ (4), and DS-ZnSe (5), DS-ZnS (6).

The luminescence spectra of the $ZnSe_{1-x}S_x$ crystals consisted of the band with the maximum in the range from 590 to 595 nm. Any sufficient differences in the luminescence properties of the samples were not revealed except for the DS-ZnS sample. For the DS-ZnS the luminescent band with a maximum at 470 nm was observed. Previously it was shown that the luminescence bands with maximums at 460 and 605 nm corresponded to the self-activated luminescences of ZnS and ZnSe crystals, respectively [29]. The difference in the X-ray induced luminescence spectra of the $ZnSe_{1-x}S_x$ samples made by SSR and DS methods can be explained by the appearance of various types of point defects responsible for energy levels involved in radiative recombination.

The optical transmission spectra of the $ZnSe_{1-x}S_x$ bulk crystals were investigated (Fig. 4). The in-line transmissions were equal to 60% at 600 nm for all crystals indicating a high optical quality of the crystals. With an increase in the sulfur content, the absorption edge shifts to the short-wavelength region [14, 25].

The relative light output and kinetic parameters of the $ZnSe_{1-x}S_x$ samples were studied (Table 3). The ZnSe(Te) crystal after annealing in zinc vapour was taken as a reference. The relative light output of the DS-$ZnSe_{1-x}S_x$ samples before annealing in zinc vapour was worse than the reference. After the annealing, the relative light output of the $ZnSe_{1-x}S_x$ samples increased. This effect can be caused by an increase of the content of zinc vacancies V_{Zn}.

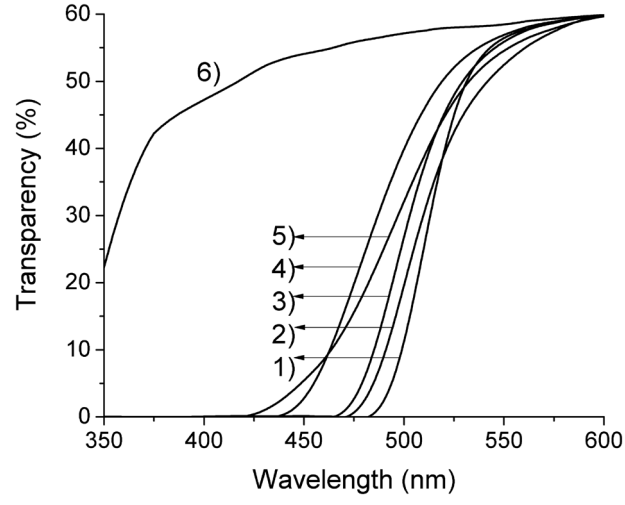

Fig. 4. Transmission spectra of DS-ZnSe (1), DS-$ZnS_{0.05}Se_{0.95}$ (2), DS-$ZnS_{0.25}Se_{0.75}$ (3), DS-$ZnS_{0.3}Se_{0.7}$ (4), DS-$ZnS_{0.4}Se_{0.6}$ (5), DS-ZnS samples (6).

Table 3. Relative value of the light output and kinetic parameters of $ZnSe_{1-x}S_x$ (x = 0.05–0.4) crystals obtained by the DS method.

Composition of sample	Light output		Decay time, τ, ms		Afterglow, % after 20 ms	
	before	after t/a Zn	before	after t/a Zn	before	after t/a Zn
ZnSe(Te)	–	1	–	–	–	–
ZnSe	0.3	0.428	–	–	–	–
$ZnSe_{0.95}S_{0.05}$	0.45	0.52–0.57	0.0026	0.011	28.2	0.08
$ZnSe_{0.75}S_{0.25}$	0.55	0.76	0.001	0.001	3.8	0.002
$ZnSe_{0.7}S_{0.3}$	0.65	1.05–1.09	0.001	0.001	6.1	0.002
$ZnSe_{0.6}S_{0.4}$	0.55–0.6	0.76–0.81	–	–	5.6	0.004
ZnS	0.53–0.56	0.47	–	–	–	–

The light output of $ZnSe_{1-x}S_x$ crystals increases with increasing the sulfur content up to $x = 0.3$ for DS-$ZnSe_{0.7}S_{0.3}$ compounds for which the light output reaches the value observed for the ZnSe(Te) 'classic scintillator'. The increase of sulfur concentrations leads to a higher content of $V_{Zn}Zn_iO_{Se}$ ternary complexes. Further increase of the sulfur content leads to the increase of defectiveness of the $ZnSe_{1-x}S_x$ crystals leading to the reduction of the light output. The highest light output was obtained for the DS-$ZnSe_{0.7}S_{0.3}$ sample due to the optimal content of ternary complexes $O_{Se}V_{Zn}Zn_i$.

In the scintillator research one is particularly interested in the scintillation decay time and afterglow. The decay time has effect on the energy resolution and speed of the detector. Afterglow determines the inertia of the scintillator and the dynamic range of the amplitudes of recorded signals. $ZnSe_{1-x}S_x$ mixed crystals have a short decay time and a low afterglow which makes these scintillators favourable for X-ray and gamma detectors (see Table 3).

The thermal stability of scintillators determines the possibility of using these scintillators in detectors operating at high intensity of radiations. The temperature dependences of relative light output were investigated (Fig. 5). The deviation of the light output in the temperature range from 80 to 350 K for the $ZnSe_{1-x}S_x$ bulk crystals does not exceed 5–8%. The temperature quenching of luminescence in the DS-$ZnSe_{0.95}S_{0.05}$ sample takes place in the 350–450 K range. Further increase of the sulfur content improves the thermal stability of our samples. The temperature quenching of luminescence in the DS-$ZnSe_{0.75}S_{0.25}$ and DS-$ZnSe_{0.6}S_{0.4}$ samples was observed in the ranges 400–500 and 430–510 K, respectively.

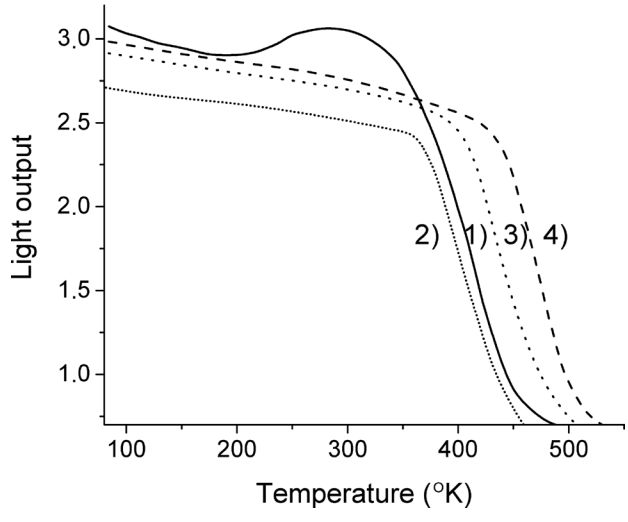

Fig. 5. Temperature dependence of the light output for ZnSe(Te) (1), DS-$ZnSe_{0.95}S_{0.05}$ (2), DS-$ZnSe_{0.75}S_{0.25}$ (3) and DS-$ZnSe_{0.6}S_{0.4}$ samples (4).

The luminescence temperature quenching of $ZnSe_{1-x}S_x$ bulk crystals (where x = 0.05–0.4) is higher than for the ZnSe(Te) crystal at the same energy of emitted photons ($h\nu \sim 2$ eV). As a result, the thermal ionization of luminescence centres for the $ZnSe_{1-x}S_x$ bulk crystals is higher than for the ZnSe(Te) [30, 31]. The temperature dependence of the light output of ZnSe(Te) crystals show the non-standard increase in the 250–350 K range. We suppose that was caused by the rearrangement of point defects in the so-called quasi-region.

Conclusions

$ZnSe_{1-x}S_x$ powders (where x = 0.07–0.97) were obtained by the solid-state reaction method. The decrease of sulfur concentration in $ZnSe_{1-x}S_x$ crystals leads to the shift of the luminescence band maximum from 500 to 530 nm up to $x = 0.33$. Further decrease of the sulfur content leads to the change in a crystallographic structure from wurtzite to sphalerite and a significant shift of the luminescence maximum to 635 nm. Such difference is caused by the change of the main type of luminescence centres from sulfur vacancies V_S to ternary complexes $O_{Se}V_{Zn}Zn_i$.

$ZnSe_{1-x}S_x$ bulk crystals were obtained by the Bridgman–Stockbarger method in the x = 0.05–0.4 range. The crystallographic studies of $ZnSe_{1-x}S_x$ bulk crystals (x = 0.05–0.4) have shown that all crystals adopt sphalerite lattices. Luminescence spectra consisted of the band with a maximum in the range from 590 to 595 nm at room temperature. The light output of $ZnSe_{1-x}S_x$ crystals increased with increasing the sulfur content up to $x = 0.3$ and reached the value of ZnSe(Te) 'classic scintillator'. At the same time, the $ZnSe_{1-x}S_x$ bulk crystals exhibit a better thermal stability as compared to that of the ZnSe(Te) crystals at the same energy of emitted photons ($h\nu \sim 2$ eV). The transparency and good luminescence properties of $ZnSe_{1-x}S_x$ bulk crystals grown by directional solidification techniques indicate the possibility of development of $ZnSe_{1-x}S_x$-based X- and γ-ray detectors.

References

[1] I.B. Mizetskaya, *Physical and Chemical Bases of Synthesis of Single Crystals of Semiconducting Solid Solutions of A^2B^6 Compound* (Naukova Dumka, Kiev, 1986) (in Russian).

[2] V.M. Koshkin, A.Y. Dulfan, N.V. Ganina, V.D. Ryzhikov, L.P. Gal'chinetskii, and N.G. Starzhinskiy, Tellurium, sulfur, and oxygen isovalent impurities in ZnSe semiconductor, Funct. Mat. **9**(3), 438–441 (2002).

[3] V.N. Tomashik, Semiconductor materials based on compounds $A^{III}B^{V}$, $A^{II}B^{VI}$, $A^{IV}B^{VI}$, in: *Inorganic Materials. V2. Materials and Technologies* (Naukova Dumka, 2009) (in Russian).

[4] V.A. Litichevskyi, A.D. Opolonin, S.N. Galkin, A.I. Lalaiants, and E.F. Voronkin, A dual-energy X-ray detector on the basis of ZnSe(Al) and LGSO(Ce) composite scintillators, Instrum. Exp. Tech. **56**(4), 436–443 (2013), https://doi.org/10.1134/S0020441213040209

[5] M. Washiyama, K. Sato, and M. Aoki, Solution growth of ZnS, ZnSe, CdS and their mixed compounds using tellurium as a solvent, J. Appl. Phys. **18**(5), 869–872 (1979), https://doi.org/10.1143/JJAP.18.869

[6] J.C. Wooley and B. Ray, Solid solution in AIIBVI tellurides, J. Phys. Chem. Solids **13**(1–2), 151–153 (1960), https://doi.org/10.1016/0022-3697(60)90135-9

[7] V.D. Ryzhikov, A.D. Opolonin, P.V. Pashko, V.M. Svishch, V.G. Volkov, E.K. Lysetskaya, and C. Smith, Instruments and detectors on the base of scintillator crystals ZnSe (Te), CWO, CsI (Tl) for systems of security and customs inspection systems, Nucl. Instrum. Methods Phys. Res. A **537**(1–2), 424–430 (2005), https://doi.org/10.1016/j.nima.2004.08.056

[8] A.G. Fischer, Preparation and properties of ZnS-type crystals from the melt, J. Electrochem. Soc. **106**(9), 838–839 (1959), https://doi.org/10.1149/1.2427507

[9] M.H. Karapet'yants, *Chemical Thermodynamics* (Khimiya, Moscow, 1975).

[10] U. Hotje, C. Rose, and M. Binnewies, Lattice constants and molar volume in the system ZnS, ZnSe, CdS, CdSe, Solid State Sci. **5**(9), 1259–1262 (2003), https://doi.org/10.1016/S1293-2558(03)00177-8

[11] K.A. Katrunov, A.L. Lalayants, V.N. Baumer, S.N. Galkin, L.P. Galchinetskii, and E.J. Brilyova, Peculiarities of scintillation materials based on ZnS–ZnTe solid solutions, Funct. Mat. **20**(3), 384–389 (2013), https://doi.org/10.15407/fm20.03.384

[12] R.C. Sharma and Y.A. Chang, Thermodynamic analysis and phase equilibria calculations for the Zn-Te, Zn-Se and Zn-S systems, J. Cryst. Growth **88**(2), 193–204 (1988), https://doi.org/10.1016/0022-0248(88)90276-X

[13] Y. Shirakawa and H. Kukimoto, The electron trap associated with an anion vacancy in ZnSe and ZnS_xSe_{1-x}, Solid State Commun. **34**(5), 359–361 (1980), https://doi.org/10.1016/0038-1098(80)90575-X

[14] S. Larach, R.E. Shrader, and C.F. Stocker, Anomalous variation of band gap with composition in zinc sulfo- and seleno-tellurides, Phys. Rev. **108**(3), 587 (1957), https://doi.org/10.1103/PhysRev.108.587

[15] N. Matsumura, M. Tsubokura, J. Saraie, and Y. Yodogawa, MBE growth of high quality lattice-matched ZnS_xSe_{1-x} on GaAs substrates, J. Cryst. Growth **86**(1–4), 311–317 (1988).

[16] B.J. Fitzpatrick, A review of the bulk growth of high band gap II–VI compounds, J. Cryst. Growth **86**(1), 106–110 (1988), https://doi.org/10.1016/0022-0248(90)90706-Q

[17] T. Homann, U. Hotje, M. Binnewies, A. Börger, K.D. Becker, and T. Bredow, Composition-dependent band gap in ZnS_xSe_{1-x}: a combined experimental and theoretical study, Solid State Sci. **8**(1), 44–49 (2006), https://doi.org/10.1016/j.solidstatesciences.2005.08.015

[18] N.G. Starzhinskiy, B.V. Grinyov, L.P. Gal'chinetskii, and V.D. Ryzhikov, *The Scintillators Based Compounds $A^{II}B^{VI}$. Preparation, Properties and Features of the Application* (Institute for Single Crystals, Kharkov, 2007) (in Russian).

[19] P. Van Ben and P.T. Tue, The role of color luminescence centers Mn, Cu, Co in the semiconductors with wide band gap ZnS, ZnO and their applications, J. Sci. Math. Phys. **24**(4), 181–187 (2008).

[20] N.B. Singh, C.H. Su, B. Arnold, and F.S. Choa, Optical and morphological characteristics of zinc selenide-zinc sulfide solid solution crystals, Opt. Mater. **60**, 474–480 (2016), https://doi.org/10.1016/j.optmat.2016.08.031

[21] R.H. Hussein, O. Pagès, F. Firszt, A. Marasek, W. Paszkowicz, A. Maillard, and L. Broch, Near-forward Raman study of a phonon-polariton reinforcement regime in the Zn(Se, S) alloy, J. Appl. Phys. **116**(8), 083511 (2014), https://doi.org/10.1063/1.4893322

[22] R.H. Hussein, O. Pagès, S. Doyen-Schuler, H. Dicko, A.V. Postnikov, F. Firszt, and O. Gorochov, Percolation-type multi-phonon pattern of Zn (Se, S): Backward/forward Raman scattering and *ab initio* calculations, J. All. Comp. **644**, 704–720 (2015), https://doi.org/10.1016/j.jallcom.2015.04.078

[23] R.H. Hussein, O. Pagès, A. Polian, A.V. Postnikov, H. Dicko, F. Firszt, and P. Fertey, Pressure-induced phonon freezing in the ZnSeS II–VI mixed crystal: phonon–polaritons and *ab initio* calculations, J. Phys. Condens. Matter. **28**(20), 205401 (2016).

[24] I. Kikuma and M. Furukoshi, Formation of defects in zinc selenide crystals grown from the melt under argon pressure, J. Cryst. Growth **44**(4), 467–472 (1978), https://doi.org/10.1016/0022-0248(78)90012-X

[25] G.D. Watkins, *Lattice Defects in II–VI Compounds* (Institute of Physics, United Kingdom, 1976).

[26] H.A. Klasens, On the nature of fluorescent centers and traps in zinc sulfide, J. Electrochem. Soc. **100**(2), 72–80 (1953), https://doi.org/10.1149/1.2781086

[27] S. Kishida, K. Matsuura, H. Fukuma, F. Takeda, and I. Tsurumi, Optical absorption bands in neutron irradiated ZnSe and $ZnS_{0.5}Se_{0.5}$, Cryst. Phys. Status Solidi B, **113**(1), K31–K33 (1982), https://doi.org/10.1002/pssb.2221130150

[28] J.R. Cutter, G.J. Russell, and J. Woods, The growth and defect structure of single crystals of zinc selenide and zinc sulpho-selenide, J. Cryst. Growth **32**(2), 179–188 (1976), https://doi.org/10.1016/0022-0248(76)90030-0

[29] M. Aven and H.H. Woodbury, Purification of II–VI compounds by solvent extraction, Appl. Phys. Lett. **1**(3), 53–54 (1962), https://doi.org/10.1063/1.1777366

[30] V.P. Glushko and V.A. Medvedev, *Thermal Constants of Substances* (Hemisphere Publishing Company, New York, 1990).

[31] D. Freik and B. Volochanska, Temperature dependencies of the heat capacity of ZnS, ZnSe and ZnSe(Te) crystals, obtained from first principles, Chem. Met. Alloys **8**, 1–4 (2015).

$ZnSe_{1-x}S_x$ DARINIŲ AUGINIMAS, STRUKTŪRA IR LIUMINESCENCINĖS SAVYBĖS

O.G. Trubaieva [a], M.A. Chaika [b], A.I. Lalayants [a]

[a] *Ukrainos nacionalinės mokslų akademijos Scintiliacinių medžiagų institutas, Charkovas, Ukraina*

[b] *Lenkijos mokslų akademijos Fizikos institutas, Varšuva, Lenkija*